



## **Cyclic elastoplastic analysis and ductility evaluation of steel braces**

I.H.P. Mamaghani<sup>1</sup>

### **Abstract**

The present paper deals with the cyclic elastoplastic large displacement behavior of steel braces. An elastoplastic finite element formulation for beam-columns, incorporating the two-surface plasticity model for material nonlinearity, is developed and implemented in the computer program FEAP used in the analysis. The formulation accounts for the important cyclic characteristics of structural steel within the yield plateau and hardening regime as well as the gradual variation of section properties in line with the spread of plasticity across the section and along the member length. The accuracy of the formulation is verified and found to be good when compared with the experiments and the results obtained from other material models. Furthermore, the effect of some important structural and material parameters on the cyclic behavior of steel braces is discussed and evaluated.

### **1. Introduction**

Steel braces are widely used as energy dissipaters in skeletal buildings, braced frames and offshore structures under extreme loading conditions, such as, severe earthquake, wind and wave motion. Therefore, an accurate cyclic analysis of such structures requires a precise method to predict cyclic behavior of bracing members. This has been the subject of intensive research work and a variety of analytical methods were developed to simulate the hysteretic behavior of steel braces in the past few decades; among others, Maison and Popov 1980, Chen and Han 1985, Mamaghani et al. 1996. The more accurate models were based on finite element method considering geometric and material nonlinearities (Clarke 1994). This method is generally applicable to many types of problems, and it requires only the member geometry and material properties (constitutive law) to be defined.

On the other hand, the stress-strain relationship used in structural analyses depends on the loading history to which the structure or structural members are subjected. Therefore, an accurate and refined constitutive law should be used to account for the general cyclic behavior of structural steel which has a characteristic yield plateau followed by strain hardening. For this purpose, based on the experimentally observed cyclic behavior of structural steel, a multiaxial

---

<sup>1</sup> Associate Professor, Department of Civil Engineering, University of North Dakota, Grand Forks, ND, 58202-8115, USA. Email: [irajmamaghani@mail.und.edu](mailto:irajmamaghani@mail.und.edu)

two-surface plasticity model (2SM) was recently developed by Mamaghani et al. 1995, and Shen et al. 1995. This model can treat accurately the cyclic behavior of structural steel within the yield plateau and hardening regime, such as the reduction and disappearance of the yield plateau, Bauschinger effect and cyclic strain hardening.

The main objective of this study is to apply the 2SM developed for material nonlinearity, in the finite element analysis, to trace cyclic elastoplastic large displacement behavior of steel braces. In what follows, first the method of analysis is briefly presented. Then, the cyclic plasticity performance of the formulation is compared with experiments as well as with results obtained from the elastic-perfectly plastic (EPP), isotropic hardening (IH) and kinematic hardening (KH) material models. It is shown that the developed formulation can predict with a high degree of accuracy the experimentally observed cyclic behavior of the steel braces.

## **2. Method of analysis**

An elastoplastic finite element formulation for beam-column of three displacements at each node, considering geometrical and material nonlinearities, was developed and implemented in the computer program FEAP (Zienkiewicz 1997) used in the analysis (Mamaghani et al. 1996). The formulation takes into account the spread of plasticity through the cross-section and along the length of member. In this approach, the member analyzed is divided into several beam-column elements along its length, and the cross-section is further subdivided into elemental areas. Each of the elemental areas is identified by, area, distance from the section centroid, residual stress and strain, and stress-strain history. The incremental stress-strain relation for each elemental area is described by the 2SM. The stress resultants of axial force and bending moment are calculated simply by summing the contribution of each elemental area over the cross-section. The full derivation of beam-column element and solution scheme are given in a work by Mamaghani 1996. In what follows, numerical results will be presented and discussed.

## **3. Numerical results**

The developed formulation was used to predict the experimentally determined hysteretic behavior of several steel braces, such as, pin-ended columns and beam-columns of strut type. The results obtained are also compared with those from bilinear EPP, KH, and IH material models. The aim is to investigate the cyclic elastoplastic performance of the steel bracing members and to compare the effect of each material model on the hysteretic behavior.

In the present study, based on the experimental results for SS400 steel, the kinematic and isotropic hardening rates are assumed as  $E_{st}'/E=1/84$  ( $E$  = Young's Modulus), which is taken equal to the slope of the line joining the initial yield point to the loading point corresponding to 5% axial strain obtained by using the 2SM (Mamaghani 1996).

### **3.1 Pin-ended Braces**

Pin-ended steel braces with solid rectangular section studied experimentally by Wakabayashi et al. (1972) are analyzed by using the developed formulation (2SM). A typical example presented here is a brace of length  $L=174$  mm, width  $b =15.45$  mm and depth  $d=14.9$  mm subjected to

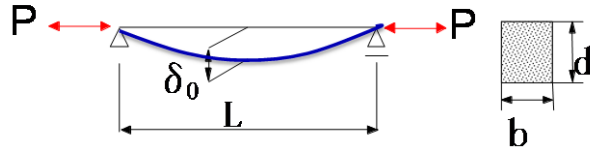


Figure 1. Pin-ended brace with a solid rectangular section:  $\lambda = 0.43$ ,  $L = 174$  mm,  $b = 15.45$  mm, and  $d = 14.90$  mm

cyclic axial load, as shown in Fig. 1. The effective slenderness ratio,  $\lambda$ , is 0.43, where  $\lambda$  is defined as:

$$\lambda = \frac{KL}{\pi r} \sqrt{\frac{\sigma_y}{E}} \quad (1)$$

in which  $L$ = length of the brace;  $K$ = effective length factor; and  $r$ = radius of gyration for the cross section. The specimen is made of SS400 steel with the material properties of Young modulus  $E=207$  GPa, yield stress  $\sigma_y=229$  MPa and yield plateau range  $\epsilon_{st}^p=0.8\%$ .

An initial imperfection of  $\delta_x = \delta_0 \sin(\pi x/L)$  is assumed in the analysis, where the initial deflection at midspan of the member  $\delta_0$ , is taken as  $0.001L$ . In the analyses, ten elements are used to discretize the member along its length and the cross-section is subdivided into 14 layers. Initial residual stress is not considered. Compressive load is applied first and it is assumed to be positive.

### 3.1.1 Cyclic behavior

Figures 2 and 3 compare the normalized axial load  $P/P_y$  versus axial displacement  $u/u_y$  and normalized axial load  $P/P_y$  versus midspan deflection  $(v + \delta_0)/d$  relationships obtained from the experiment (Wakabayashi et al. 1972) and analysis using the 2SM as well as the EPP, KH and IH material models, respectively. The normalized maximum compressive load  $P_{max}/P_y$ -number of cycles for the column is shown in Figure 4. Here,  $P_y$  is the squash load;  $u_y$  is the yield displacement in tension for the brace.

Fig. 2(a) for the experiment shows that after initial buckling the load carrying capacity of the brace rapidly decreases and it is accompanied by yielding of the section at midspan of the brace. In subsequent cycles a reduction in the buckling load capacity is observed. This reduction can attribute to the residual lateral displacement at midspan of the brace, see Fig. 2(b), and the Bauschinger effect of the material. With reference to Figs. 2, 3 and 4, the following observation can be made.

The initial buckling load, see Figs. 2(a), 3(a) and 4, is slightly higher in the experiment than that predicted by the analyses using different material models. This may be due to the experimental boundary conditions (unavoidable friction at the hinged supports) and the assumed initial imperfection in the analysis. (2) The significant features of the hysteretic loops in Figs. 2(a) and 3(a) is that all of the models except the 2SM give the second and subsequent buckling load

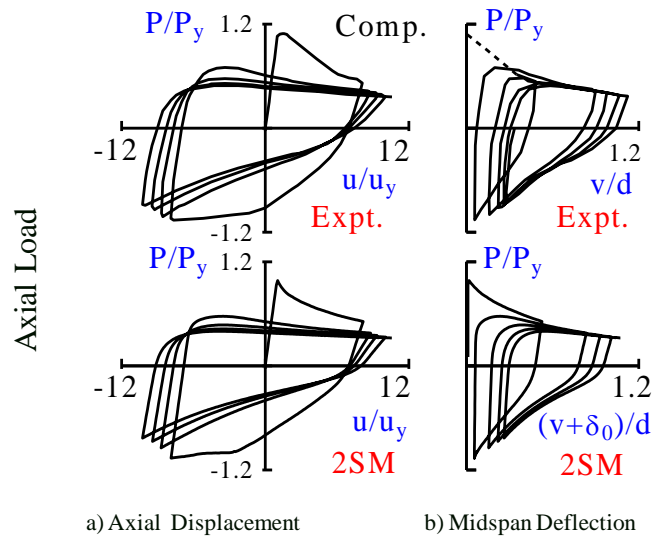


Figure 2. Comparison between experimental and predicted hysteretic loops using the 2SM

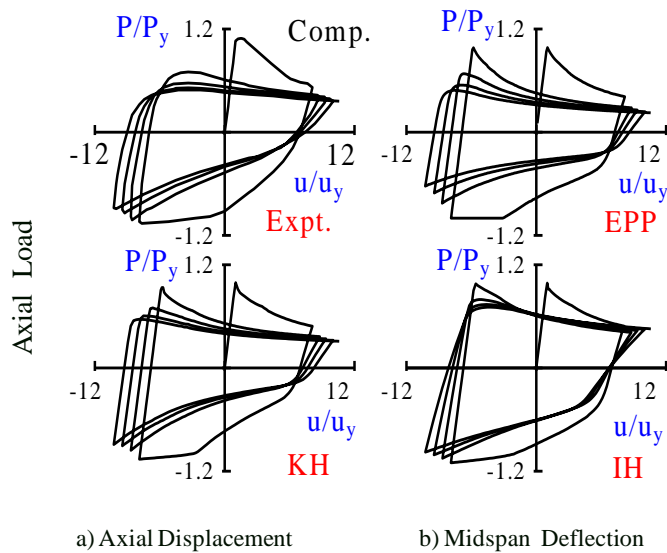


Figure 3. Comparison between experimental and predicted hysteretic loops using EPP, KH and IH material models

capacities higher than those of the experiment (see also Fig. 4). The reasons are: (a) The EPP and IH models do not consider the reduction of the elastic range due to plastic deformation (Bauschinger effect); and for the KH model the size of the elastic range is taken to be constant which does not represent the actual behavior of structural steel (Mamaghani et al. 1995). In the case of the 2SM, Bauschinger effect is taken into account accurately through updating the size of yield surface as a function of the effective plastic strain (EPS) range  $\bar{\epsilon}_{st}^p$  (Shen et al. 1995), which has the effect of softening the hysteresis curve (reduction in stiffness), leading to a lower value of the buckling load capacity; (b) the 2SM correctly treats the yield plateau and cyclic strain hardening of the material. This leads to an accurate prediction of the midspan deflection for the brace, see Fig. 2(b), since the residual deflection of the brace at the end of the previous

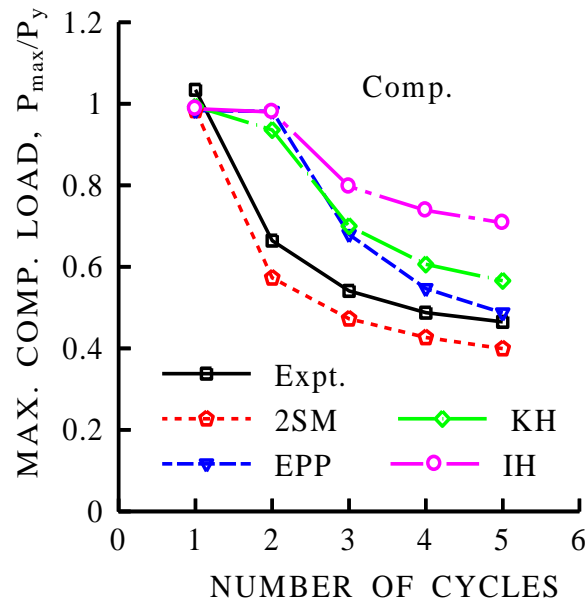


Figure 4. Normalized maximum compressive load  $P_{max}/P_y$  versus number of cycles

tensioning has a large effect on the buckling load capacity and subsequent cyclic behavior. As can be noticed from Figs. 2(b) and 3(b), the progress of buckling is different for each material model. In case of the IH model, in spite of large progress in buckling, see Fig. 3(b), the buckling load does not decrease significantly due to the larger cyclic strain hardening.

Figures 5 and 6 show the experimental results (Wakabayashi et al. 1972) and prediction by the 2SM for two pin-ended braces with solid rectangular sections of  $\lambda = 0.85$  and 1.28, respectively. Similar to the previous example, the results in Fig. 5 indicate that the smooth trend of buckling load degradation and the overall hysteretic response are satisfactorily simulated by the 2SM.

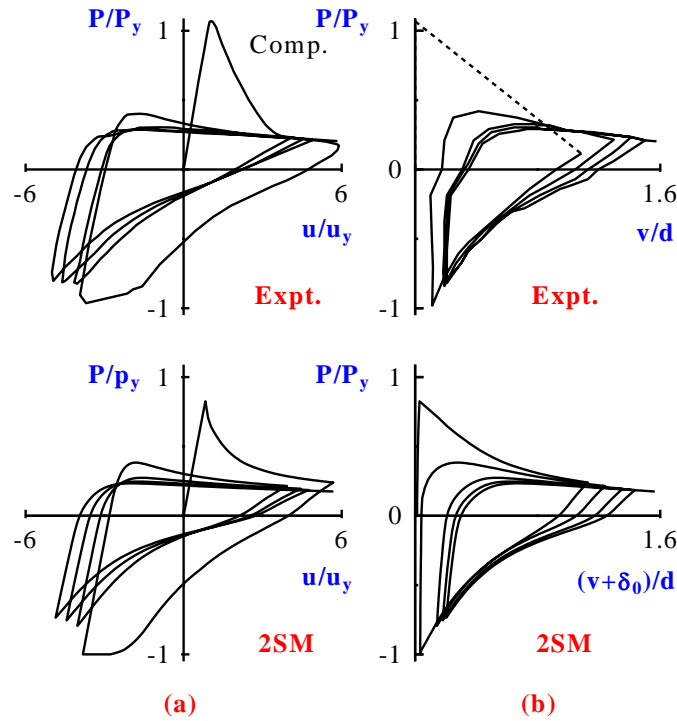


Figure 5. Comparison between experimental and predicted hysteretic loops by the 2SM:  
 $\lambda=0.85$

### 3.2 Energy Absorption Capacity

Energy absorption through hysteretic damping can reduce the amplitude of seismic response and, thereby, reduce the ductility demand on the structures. Therefore, it is of great interest in seismic design. In order to account for the displacement history to which the inelastic performance of a structure is highly sensitive, normalized energy absorption  $\bar{E}$ , defined as:

$$\bar{E} = \frac{1}{E_y} \sum_{i=1,n} E_i \quad (2)$$

Where,

$$E_y = \frac{1}{2} P_y u_y \quad (3)$$

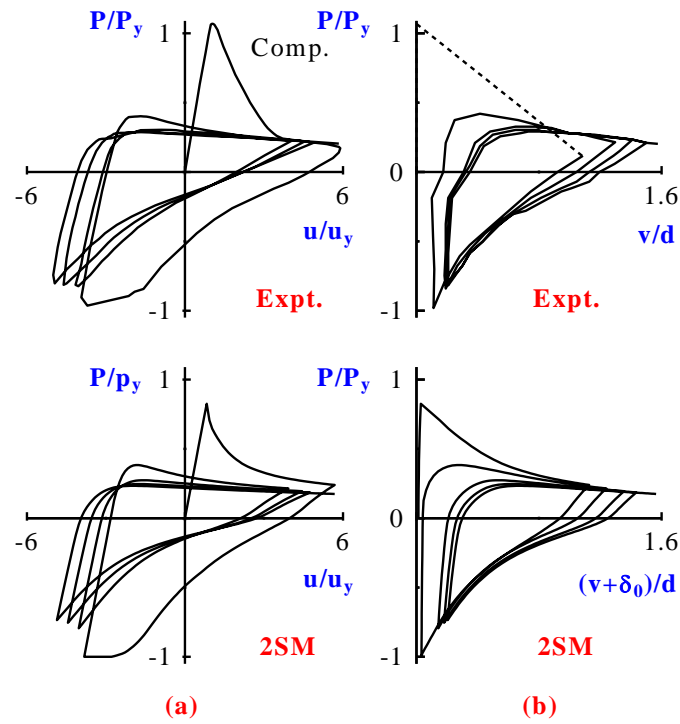


Figure 6. Comparison between experimental and predicted hysteretic loops by the 2SM:  $\lambda=1.28$

The normalized energy absorption through hysteretic damping is considered to be a more objective measure of the cyclic inelastic performance of a member. In the Eq. (2),  $E_i$  = energy absorption in the  $i$ -th half-cycle,  $n$  = number of half-cycles (one half-cycle is defined from any zero axial load to the subsequent zero axial load).

Using the above definitions, Figs. 7 and 8 compare the normalized cumulative energy absorption capacity,  $\bar{E}$  versus the number of half-cycle  $n$ , obtained from experiment and analysis using the 2SM, for  $\lambda = 0.43, 0.85$  and  $1.28$ . The results in Figs. 7 and 8 indicate a good agreement between the experiment and prediction by the 2SM.

The results in Figs. 2-8 show that the hysteretic behavior of the brace is affected by its slenderness ratio. Braces with small slenderness ratio generate fuller, more rounded curves than more slender braces (see Figs. 2-6) and consequently absorb more energy, see Fig. 7. All of these effects are simulated well using the developed formulation (2SM), see Figs. 2-8.

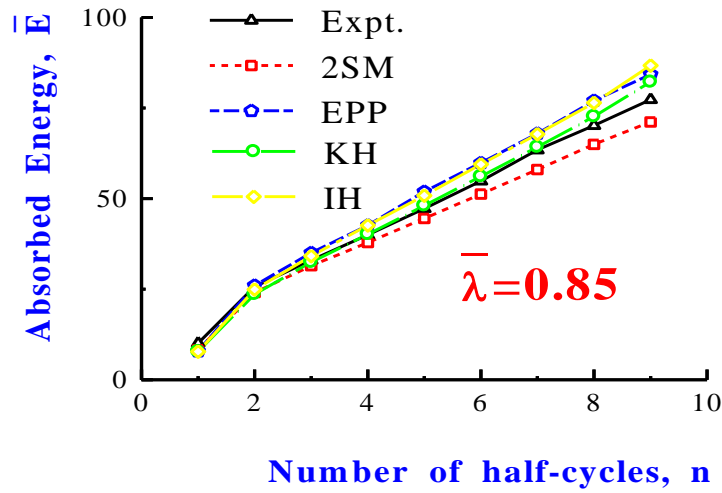


Figure 7. Comparison of absorbed energy versus material models

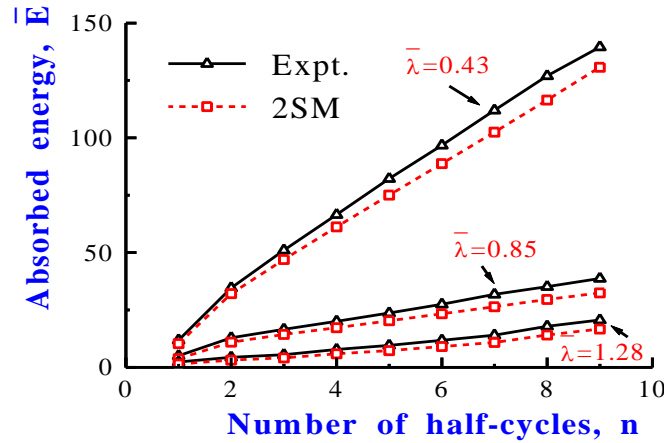


Figure 8. Comparison of absorbed energy versus brace slenderness ratio

### 3.3 Braces of Strut Type

Braces of a strut type are fixed-ended bracing members subjected to constant lateral loads  $Q$  and cyclic axial displacements  $u$ , as shown in Fig. 9. These members are widely used in the offshore steel platforms and space truss structures. Using the developed formulation (2SM), a series of numerical studies on the cyclic behavior of struts is carried out and the results are compared with the test data (Sherman 1979).

Figs. 10 and 11 show axial load-axial shortening and axial load-midspan deflection for two typical examples, with material constants, dimensions, boundary and loading conditions as shown. The specimens have effective slenderness ratio of  $\lambda = 0.87$  and are subjected to lateral load ratios of  $Q/Q_y = 0.4$  and  $0.1$ , respectively. Where  $Q$  is the lateral point load and  $Q_y$  is the value of  $Q$  which causes first yield in a strut with no axial load applied. An initial imperfection and residual stress are not considered in these examples. After applying the constant lateral load



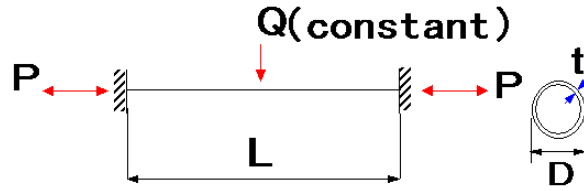


Figure 9. Braces of strut type ( $\lambda = 0.87$ ,  $L = 5720$  mm,  $D = 114$  mm,  $t = 2.3$  mm,  $E = 200$  GPa,  $\sigma_y = 289$  MPa,  $Q_y = 9.12$  kN)

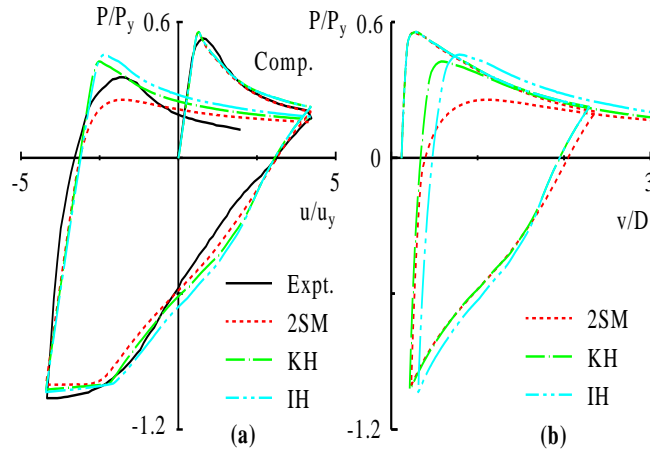


Figure 10. Comparison between predicted and experimental results:  $Q=0.4Q_y$   
 (a) normalized axial load  $P/P_y$ -axial displacement  $u/u_y$ ; (b) normalized axial load  $P/P_y$ , midspan deflection  $v/D$ .

of  $Q$  at midspan, the specimen is first loaded in compression. The 2SM, EPP, KH and IH models simulate the experiments quite well in the pre-and post-buckling stages of axial deformation, see Figs. 10(a) and 11(a). Upon reversal of the axial deformation in tension and reloading in compression, the 2SM provides a relatively closer fit to the test data as compared with the other models, owing to the same reasons mentioned in the previous examples. As shown in Figs. 10 and 11, except for the 2SM the buckling load capacity in the second cycle is predicted higher than that of the experiments.

#### 4. Conclusions

This paper was concerned with the cyclic elastoplastic large displacement behavior of steel braces. An elastoplastic finite element formulation for beam-columns, employing the 2SM for material nonlinearity, was developed and used in the analysis. The effect of some important structural and material parameters on cyclic behavior of steel braces was pointed out and evaluated. It was shown that the use of the EPP, KH and IH material models in the cyclic analysis of steel braces may lead to an erroneous estimate of cyclic behavior (load carrying

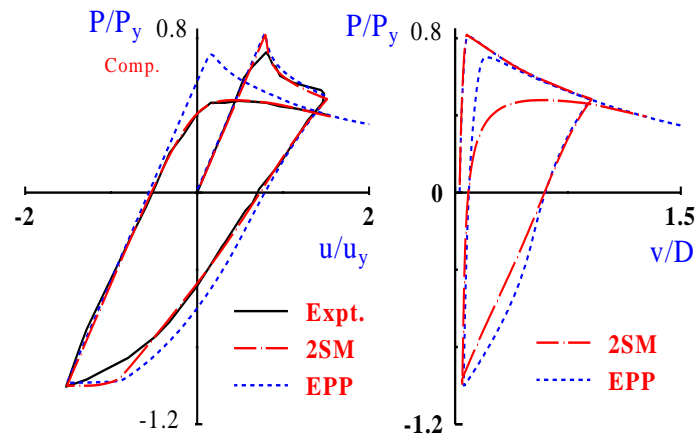


Figure 11. Comparison between predicted and experimental results:  $Q = 0.1Q_y$   
 (a) normalized axial load  $P/P_y$ -axial displacement  $u/u_y$ ; (b) normalized axial load  $P/P_y$  - midspan deflection  $v/D$ .

capacity and energy absorption capacity) in contrast to the 2SM. That is, the 2SM can be used in the analysis of steel braces more confidently.

## References

- Chen, W. F., Han, D. J.(1985), ``Tubular members in offshore structures'', Pitman Publishing Inc.
- Clarke, M. J. (1994), ``Plastic-zone analysis of frames'', Advanced analysis of steel frames, edited by Chen, W. F. and Toma, S., CRC press, Boca Raton, FL, 259-319.
- Maison, B. F. and Popov, E. P. (1980), ``Cyclic response prediction for braced steel frames'', J. Struct. Engng, ASCE, 106(7), 1401-1416.
- Mamaghani, I. H. P., Shen, C., Mizuno, E., Usami, T. (1995), ``Cyclic behavior of structural steels. I: Experiments''. Journal of Engineering Mechanics, ASCE, 121(11), 1158-1164.
- Mamaghani, I. H. P., Usami, T. and Mizuno, E. (1996), ``Inelastic large deflection analysis of steel structural members under cyclic loading''. Engineering Structures, UK, 18(9), 659-668.
- Mamaghani, I.H.P.(1996), ``Cyclic elastoplastic behavior of steel structures: Theory and experiments'', Doctoral Dissertation, Dept. of Civil Engineering, Nagoya University, Nagoya, Japan.
- Shen, C., Mamaghani, I. H. P., Mizuno, E. and Usami, T. (1995), ``Cyclic behavior of structural steels. II: Theory''. Journal of Engineering Mechanics, ASCE, 121(11), 1165-1172.

Sherman, D. R. (1979), "Post local buckling behavior of tubular strut type beam-columns: An experimental study". Report to shell oil company, University of Wisconsin-Milwaukee.

Wakabayashi, M., Matsui, C. and Mitani, I. (1972), "Experimental studies on the elastic-plastic stability of steel frames, part 4. Trans. of Arch. Inst. of Japan, No. 195, 25-37.

Zienkiewicz, O. C. (1977), "The Finite Element Method". 3rd Ed., McGraw-Hill, New York.